

## Discriminative study of genetically diverse carbonate rocks in the northwestern Pikwitonei granulite domain and Split Lake block, central Manitoba (parts of NTS 63P11, 12, 64A1)

by J.A. Macdonald<sup>1</sup>, A.R. Chakhmouradian<sup>1</sup>, C.G. Couëslan and E.P. Reguir<sup>1</sup>

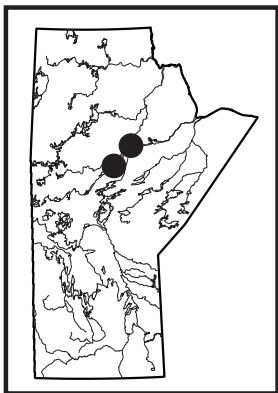
<sup>1</sup> Department of Geological Sciences, University of Manitoba, 125 Dysart Road, Winnipeg, MB R3T 2N2

### In Brief:

- Genetically diverse types of carbonate rocks identified in the Split Lake block and Pikwitonei granulite domain
- Possible carbonatite discovered at Split Lake; may indicate potential for rare metals
- New petrogenetic interpretations of carbonate rocks help constrain the geodynamic evolution of the Superior Boundary zone

### Citation:

Macdonald, J.A., Chakhmouradian, A.R., Couëslan, C.G. and Reguir, E.P. 2017: Discriminative study of genetically diverse carbonate rocks in the northwestern Pikwitonei granulite domain and Split Lake block, central Manitoba (parts of NTS 63P11, 12, 64A1); *in* Report of Activities 2017, Manitoba Growth, Enterprise and Trade, Manitoba Geological Survey, p. 30–41.



### Summary

Correct petrogenetic interpretation of carbonate rocks is important for geodynamic reconstruction of structurally complex terranes, and because these rocks can potentially host a variety of mineral resources (e.g., base metals, Mo and W in skarns; rare earths and Nb in carbonatites; diamonds in kimberlites). Carbonate minerals are strongly susceptible to metamorphic decarbonation, and textural and geochemical re-equilibration. Consequently, carbonate rocks of different origins may appear macroscopically similar in metamorphic terranes and require detailed analysis of their trace-element and isotopic compositions to identify their origin. Ten occurrences of carbonate rock in the high-grade Split Lake block and Pikwitonei granulite domain of northern Manitoba are the focus of the present study. Petrographic and quantitative analyses of calcite and dolomite from these rocks were carried out to aid in the determination of their origin. A potential new locality of carbonatite magmatism at Split Lake is identified.

### Introduction

Carbonatites are rare mantle-derived igneous rocks that are strongly susceptible to subsolidus processes capable of completely overprinting their primary petrographic features (Chakhmouradian et al., 2016b). Consequently, identification of carbonatites can be difficult, especially in heavily deformed terranes. Altered basalts, hydrothermal veins, supracrustal sediments and carbonatites can all show similar petrographic characteristics after being subjected to even low-grade metamorphism. Furthermore, extrusive and shallow intrusive carbonatites can be easily confused with other carbonate-rich rocks, such as kimberlites and ultramafic lamprophyres, which will have implications for mineral exploration (Chakhmouradian et al., 2009a). Additionally, a correct interpretation of carbonate rocks is essential for geodynamic reconstruction by providing a tectonic context.

Because strongly deformed carbonate rocks are commonly misinterpreted (Le Bas et al., 2002, 2004), nonpetrographic considerations must be taken into account to identify rocks of igneous origin. The presence of pyrochlore suggests a carbonatitic origin (Le Bas et al., 2002), whereas anorthite, scapolite or spinel are more consistent with a sedimentary source (Le Bas et al., 2002). Igneous carbonate is characterized by a high Sr content and typically shows an enrichment in light rare-earth elements (LREE; Chakhmouradian et al., 2016b). However, metamorphic reactions can drastically change the mineralogy (Chakhmouradian et al., 2015), and the distribution of REE in igneous carbonate can be modified by supergene or magmatic processes (Xu et al., 2007; Chakhmouradian et al., 2016a). Element ratios are more robust petrogenetic indicators in that Eu and Ce anomalies are generally lacking in carbonatites, whereas their Y/Ho value approaches that of the primitive mantle (Le Bas et al., 2002, 2004; Chakhmouradian et al., 2016a). Magmatic carbonates generally plot in the ranges  $\delta^{13}\text{C}_{\text{V-PDB}} = -4\text{‰}$  and  $-8\text{‰}$  and  $\delta^{18}\text{O}_{\text{V-SMOW}} = +6\text{‰}$  and  $+10\text{‰}$  on stable-isotope discrimination diagrams (Taylor et al., 1967; Demény et al., 2004). However, various syn- to postemplacement processes can affect the isotopic composition of carbonatites (Demény et al., 2004).

To date, several localities of carbonate rocks of uncertain origin have been reported from the Pikwitonei granulite domain (PGD) and Split Lake block (SLB) of northern Manitoba (Figure GS2017-4-1). With a few exceptions, most these occurrences were first documented in detail by Couëslan (2013, 2014). The present contribution provides a preliminary assessment of 10 significant carbonate-rock occurrences in the PGD and SLB based on the above criteria.

### Regional geology

The Superior boundary zone (SBZ) is a transitional structural domain between the Archean continental rocks of the Superior province to the south and east, and the Paleoproterozoic juvenile

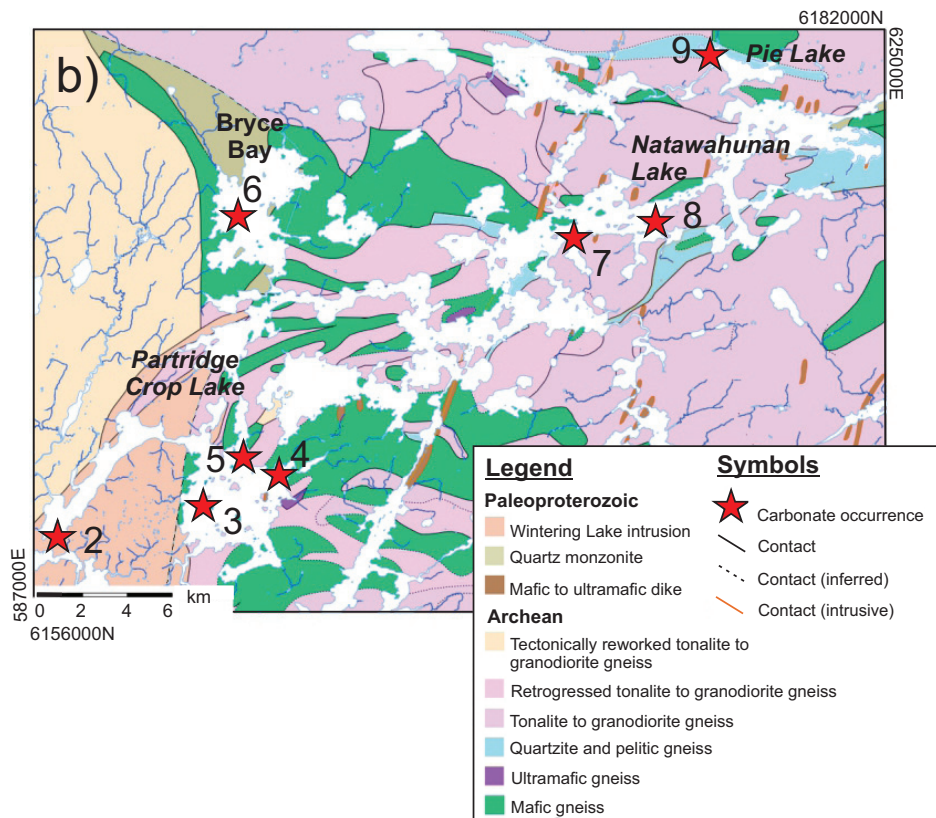
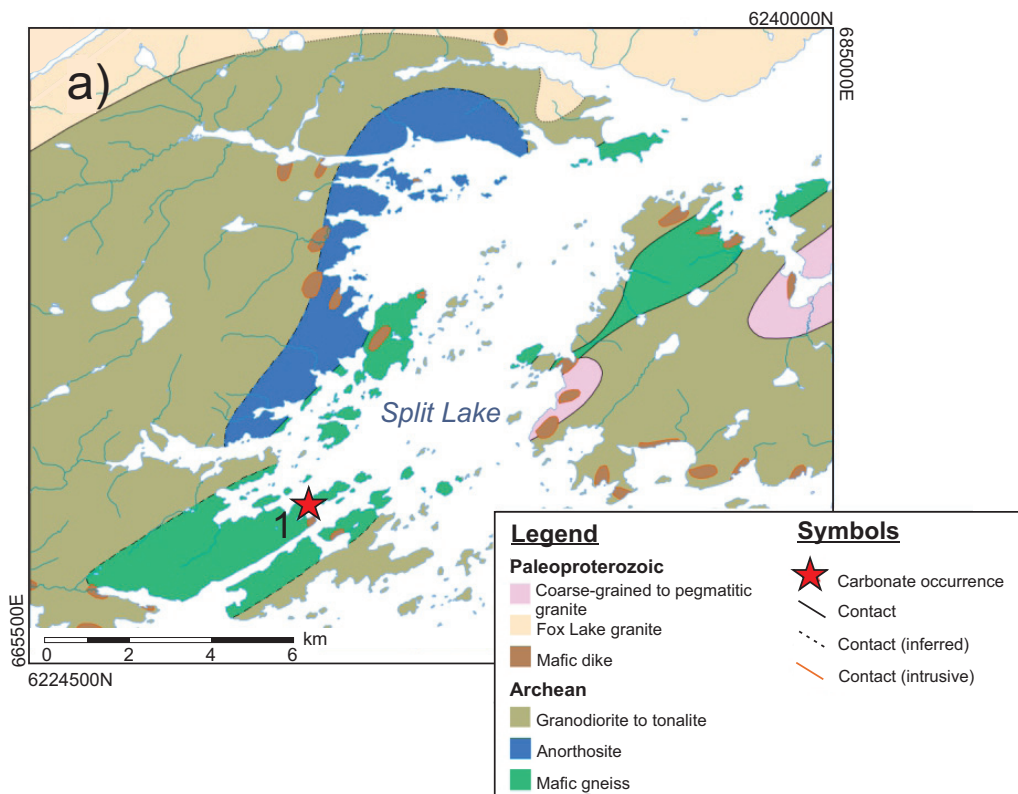


**Figure GS2017-4-1:** Simplified geological maps of the Split Lake (a) and Partridge Crop–Natawahunan Lake (b) areas (abbreviated PCL and NL, respectively), showing the locations of the studied occurrences of carbonate rocks: 1, Split Lake; 2, PCL-01; 3, PCL-02; 4, PCL-03; 5, PCL-04; 6, Bryce Bay; 7, NL-01 and NL-02 (located ~200 m apart and represented by a single star); 8, NL float; 9, Pie Lake.

volcanic arc and associated metasedimentary rocks of the Reindeer zone to the north and west. The PGD and SLB represent mid- to deep-crustal rocks of the Superior craton and are separated from each other by shear zones (Hartlaub et al., 2005; Kuiper et al., 2011). The majority of the examined occurrences are located in the PGD, at Partridge Crop and Natawahunan Lakes, with one site in the SLB, at Split Lake (Figure GS2017-4-1).

### ***Split Lake block***

The SLB is a geologically distinct terrane bounded by the Assean Lake shear zone to the north and the Aiken River shear zone to the south. It consists largely of metamorphosed igneous rocks with protoliths generated through multiple episodes of magmatism; age relations among these units are unclear (Böhm et al., 1999). Archean rocks in this area consist of supracrustal metapelite, mafic-ultramafic granulite and an igneous complex consisting of anorthosite, gabbro and mafic tonalite. The Archean rocks are often present as disrupted rafts in younger felsic intrusions (Böhm et al., 1999). The same authors also noted that the SLB was isolated from significant Paleoproterozoic deformation. The high-grade terrane is crosscut by weakly metamorphosed Paleoproterozoic mafic dikes and intruded in the north by the Fox Lake granite (ca. 1825 Ma; Heaman et al., 2011). It is hypothesized that the SLB and the PGD share their metamorphic histories at ca. 2.7 Ga (Böhm et al., 1999), but the PGD was unaffected by regional amphibolite-facies retrogression (Hartlaub et al., 2003).

### ***Pikwitonei granulite domain***

The Pikwitonei granulite domain (PGD) is an integral part of the Northern Superior superterrane and one of the largest and best-preserved high-grade Neoproterozoic terranes in the world (Heaman et al., 2011; Couëslan, 2013). The PGD grades into the Thompson Nickel belt (TNB) to the west, and is separated from the SLB to the north by the Aiken River shear zone and from the typical granite-greenstone belts to the south and east by an orthopyroxene isograd (Hartlaub et al., 2005; Heaman et al., 2011; Kuiper et al., 2011). The gradual transition from low-grade rocks to their high-grade equivalents in the PGD represents a continuous oblique crustal cross-section (Heaman et al., 2011). The PGD consists largely of intermediate to felsic, orthopyroxene-bearing gneisses and migmatites, mafic granulites and amphibolites (Heaman et al., 2011). At least four episodes of metamorphism and two major phases of deformation are documented in the PGD. The prominent east-trending  $S_1$  metamorphic layering and isoclinal folding were developed during the first phase ( $D_1$ - $M_1$ ), which occurred under upper amphibolite- to lower granulite-facies conditions and caused widespread anatexis (Heaman et al., 2011; Couëslan, 2013). This was followed by phase  $D_2$ , which generated a strong quartz fabric ( $S_2$ ) that is axial planar to minor isoclinal folding

(Couëslan, 2016). Granulite-facies metamorphism ( $M_2$ ) resulted in the formation of leucosomes attenuated with  $S_2$ , which suggests that they developed synchronously with, or were outlasted by,  $D_2$  (Couëslan, 2016). Paleoproterozoic deformation events caused amphibolite-grade retrogression that increases in intensity toward the TNB.

Partridge Crop Lake is located in the transition zone between the PGD and SBZ, and thus experienced Paleoproterozoic deformation and retrograde metamorphism at amphibolite-facies conditions (Heaman et al., 2011; Couëslan, 2016). The bedrock geology consists of felsic and mafic Archean gneisses interspersed with metamorphosed supracrustal rocks and intruded by granitoids of Paleoproterozoic age (Couëslan, 2013). The Wintering Lake granite dominates the southwestern portion of the area and has been dated at  $1846 \pm 8$  Ma and  $1822 \pm 5$  Ma (Machado et al., 2011a, b). Mafic and ultramafic dikes crosscut the regional gneissosity in two main orientations, and are tentatively interpreted to represent the Molson dike swarm (ca. 1880 Ma) and possibly an older, east-northeast-trending group of unknown provenance (ca. 2090–2070 Ma; Heaman and Corkery, 1996; Halls and Heaman, 2000; Couëslan, 2013). Peak metamorphic conditions in the Partridge Crop Lake area are approximated at 790–850°C and 8.3–10.7 kbar (Paktunç and Baer, 1986; Mezger et al., 1990).

Natawahunan Lake is located in the western extent of the PGD. The bedrock geology of this area is dominated by granulite- and amphibolite-facies assemblages that were retrogressively metamorphosed to amphibolite- and greenschist-facies assemblages (Weber, 1978; Böhm, 1998; Heaman et al., 2011; Couëslan, 2016). Here, the basement comprises schollen enderbite and orthopyroxene-bearing felsic gneisses (Couëslan, 2016). Other units include mafic and garnet-bearing gneisses and metasedimentary rocks (Couëslan, 2016). A Paleoproterozoic shear zone runs the length of Natawahunan Lake (Couëslan, 2016). Veins consisting of quartz and subordinate carbonate and lined with chlorite are associated with shear zones of Hudsonian age and areas of intense carbonate-chlorite-sericite alteration (Couëslan, 2016). Peak metamorphic conditions at Natawahunan Lake reached 800–830°C and 6.5–8 kbar (Paktunç and Baer, 1986; Mezger et al., 1990).

### **Carbonate rocks in northeastern Manitoba**

The stable C and O isotope data and major- and trace-element compositions of calcite discussed below, as well as the detailed petrographic descriptions of the carbonate rocks, were collected during the present study. Selected occurrences of carbonate rock contain calcite-dolomite pairs that allow the temperature of dolomite equilibration to be calculated (Anovitz and Essene, 1987). An in-depth description of the analytical techniques used is provided with the geochemical data in Data Repository Item DRI2017005 (Macdonald et al., 2017)<sup>2</sup>.

<sup>2</sup> MGS Data Repository Item DRI2017005, containing the data or other information sources used to compile this report, is available to download free of charge at <http://www2.gov.mb.ca/itm-cat/web/freedownloads.html>, or on request from [minesinfo@gov.mb.ca](mailto:minesinfo@gov.mb.ca) or Mineral Resources Library, Manitoba Growth, Enterprise and Trade, 360–1195 Ellice Avenue, Winnipeg, Manitoba, R3G 3P2, Canada.

## Split Lake

A sample of apatite-bearing pink carbonate rock (36-77-435-1) was collected at Split Lake and archived by T. Corkery in 1977. This locality was revisited by the authors in 2016 (GS2017-4-1a). Although the original outcrop was not found, a carbonate rock was recognized (Figure GS2017-4-2a). This rock is hosted within a foliated granodiorite, has a dark-green weathered appearance and crosscuts the regional foliation in thin (~4 cm wide) bands in different orientations. The bands are enveloped in a light-green alteration halo several centimetres wide (Figure GS2017-4-2a) and crosscut by felsic veins. Coarse-grained calcite was sampled from one of the bands (Green Bay calcite) and studied along with the material collected by T. Corkery.

Sample 36-77-435-1 consists predominantly of calcite, diopside and apatite. Accessory phases include xenocrystic plagioclase and trace amounts of allanite, pyrite and tremolite. Calcite shows 'patchy' zoning in backscattered-electron scanning electron microscope (BSE) images (Figure GS2017-4-2b), consisting of irregularly shaped core areas that show a relatively high average atomic number (AZ) and areas of lower AZ developed along grain margins and cleavage planes. Some calcite crystals contain small subhedral apatite inclusions (Figure GS2017-4-2b). Apatite occurs as grains measuring 0.5–3.0 mm across, both in the calcite mesostasis and in xenoliths that contain interstitial allanite (Figure GS2017-4-2c). Plagioclase ( $An_{31-33}$ ) is present in highly digested xenoliths, where it is replaced metasomatically by an aggregate of albite ( $An_9$ ) and muscovite. Plagioclase xenocrysts also exhibit reaction rims zoned from clinzoisite at the xenolith margin to epidote and then allanite in contact with the surrounding calcite.

Major-element compositions of calcite form two populations: one containing no detectable Mg, Mn or Fe and low  $\Sigma$ REE, and the other characterized by higher levels of Mg, Mn, Fe and REE. Both populations are enriched in Sr with respect to the rest of the sample suite (Figure GS2017-4-3a), and the Y/Ho ratios are close to the primitive-mantle value (Figure GS2017-4-3b). The high-AZ variety is enriched in LREE relative to heavy REE (HREE), as reflected in their chondrite-normalized  $(La/Yb)_{CN}$  values, whereas the low-AZ variety shows relative depletion in

LREE (Figure GS2017-4-4). The normalized profiles of both varieties are flat and lack any Eu anomaly.

The Green Bay calcite contains abundant microscopic inclusions of dolomite, interpreted to have formed by exsolution, and scarce fragments of oscillatory-zoned ankerite and Fe-rich dolomite; both calcite and dolomite show enrichment in Mn. In contrast to sample 36-77-435-1, the Green Bay material contains little Sr or REE (Figure GS2017-4-3a). This calcite has a mantle-like Y/Ho ratio ( $25 \pm 2$ ), similar to that in sample 36-77-435-1, but shows extreme enrichment in HREE ( $[La/Yb]_{CN} \ll 0.01$ ; Figure GS2017-4-4) where the LREE are at or below detection.

Sample 36-77-435-1 is confidently identified as intrusive calcite carbonatite (sövite), as it shows mineralogical, trace-element and stable-isotope characteristics (Figure GS2017-4-5) consistent with primary igneous carbonate: the presence of allanite and apatite; the absence of a Eu anomaly and a mean Y/Ho value of  $26 \pm 3$ ; enrichment of the calcite in Sr, LREE and light C and O isotopes (as reflected in its  $\delta^{13}C_{V-PDB}$  and  $\delta^{18}O_{V-SMOW}$  values; see Figure GS2017-4-5 for definition of these abbreviations); and 'patchy' zoning in calcite indicative of Sr and REE removal by late-stage fluids (Demény et al., 2004; Le Bas et al., 2004; Chakhmouradian et al., 2016a). Interestingly, this sample is mineralogically and geochemically similar to sövite from Paint Lake, some 120 km southwest of Split Lake in the SBZ (Couëslan, 2008; Chakhmouradian et al., 2009b).

The crosscutting relationships of the carbonate rocks observed on Split Lake in 2016 and their associated green alteration envelope, potentially representing the fenitization process, are consistent with carbonatitic magmatism (Le Bas, 2008). The low Sr and REE abundances in the Green Bay calcite argue against an igneous origin; however, stable C and O isotope data plot in the primary igneous field (Figure GS2017-4-5) and it has been shown that deformation and hydrothermal reworking of igneous carbonates can result in the removal of Sr and REE, generating a variety of REE distribution patterns (Chakhmouradian et al., 2016a).

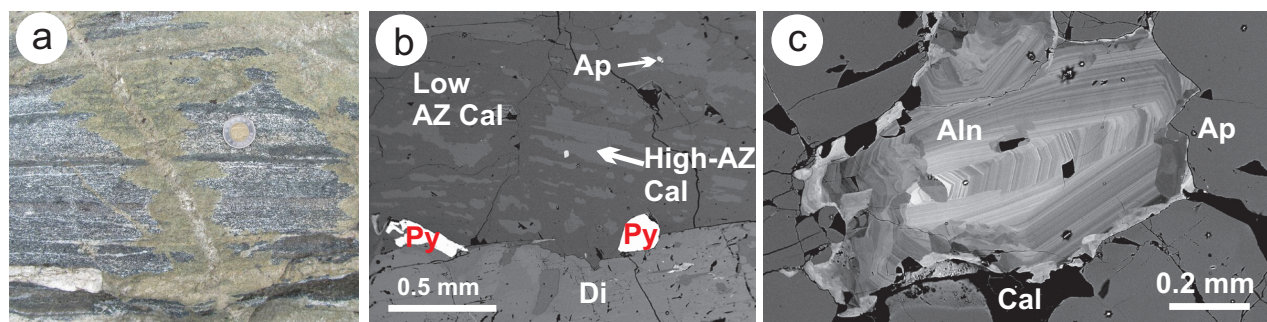


**Figure GS2017-4-2:** Structural and textural relations of the carbonate rocks at Split Lake: **a)** carbonate vein crosscutting gneissic host with associated alteration halo (potentially representing fenitization); **b)** backscattered-electron scanning electron microscope (BSE) image showing zoning in the calcite from sample 36-77-435-1; note presence of apatite; **c)** BSE image showing zoned allanite interstitial to apatite in apatite-rich xenolith. Abbreviations: Aln, allanite; Ap, apatite; AZ, average atomic number; Cal, calcite; Di, diopside, Py, pyrite.

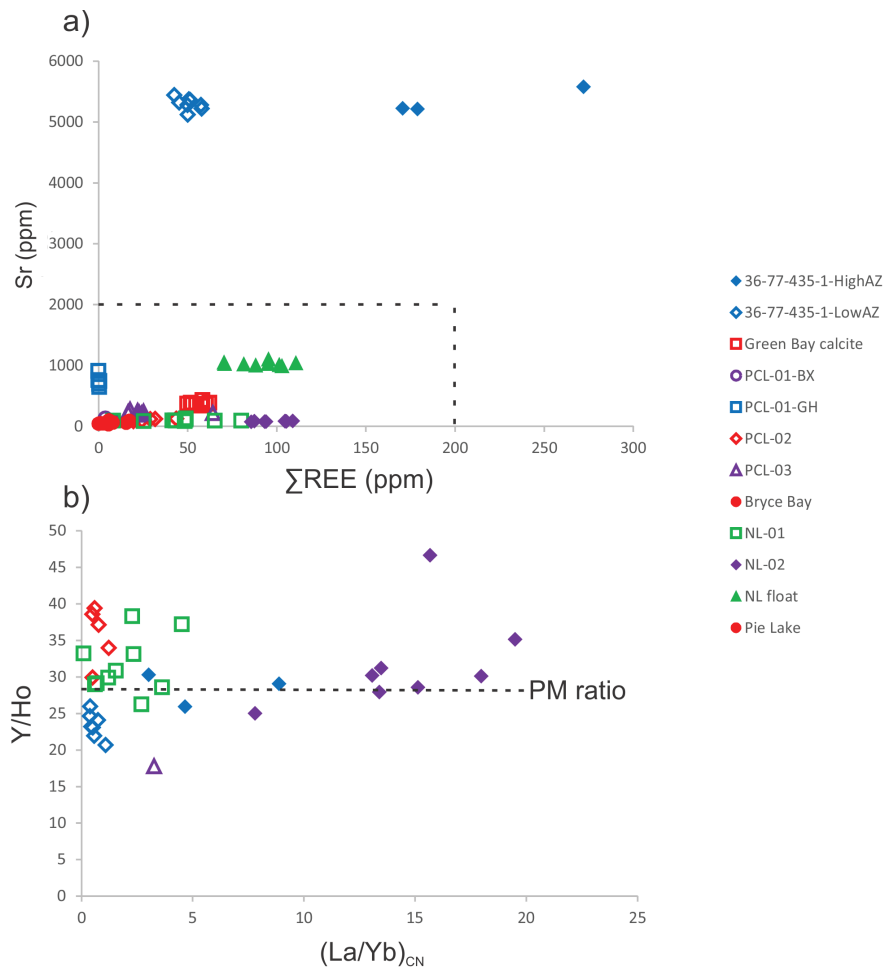


**Figure GS2017-4-3:** Trace-element compositions of calcite from the studied carbonate rocks. Dashed box in lower left corner of (a) indicates the inferred Sr and ΣREE contents of sedimentary carbonates (Chakhmouradian et al., 2009b). Dashed line in (b) represents the Y/Ho ratio of the primitive mantle; selected occurrences of carbonate rock have been omitted from (b) because one or more of Y, Ho, La or Yb were undetected, so the plotted ratios could not be calculated. Abbreviations: AZ, average atomic number; BX, brecciated variety of carbonate rock at outcrop PCL-01; GH, granite-hosted calcite at outcrop PCL-01; PM, primitive mantle.

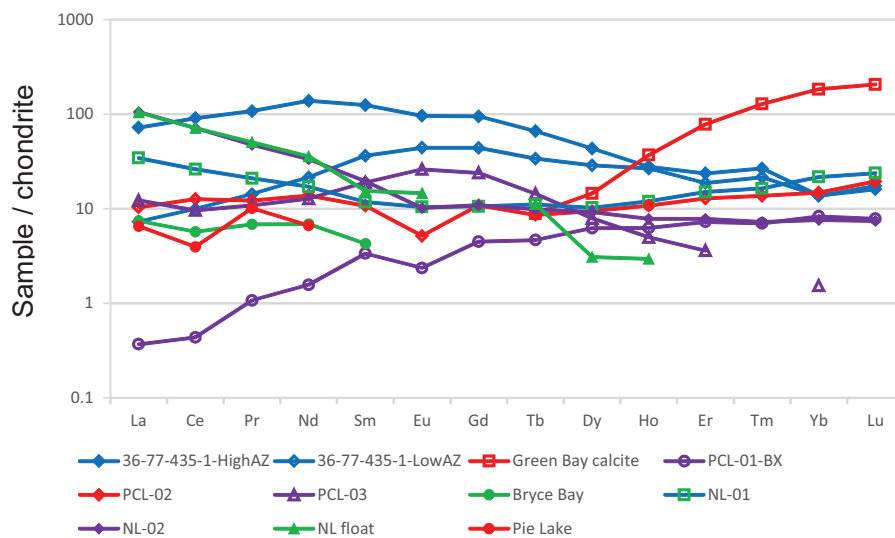


**Figure GS2017-4-4:** Average chondrite-normalized REE profiles of calcite in selected carbonate rocks from this study (normalization values from Anders and Grevesse, 1989). Granite-hosted calcite of outcrop PCL-01 has been omitted because the REE were not confidently detected. Abbreviations: BX, brecciated variety of carbonate rock at outcrop PCL-01.

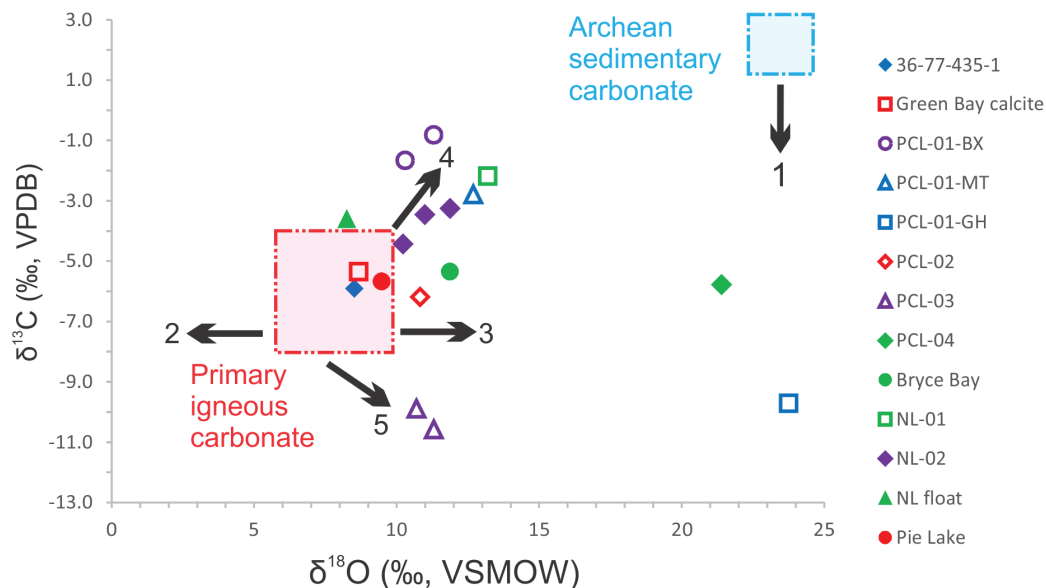


**Figure GS2017-4-5:** Carbon and oxygen stable-isotope compositions of calcite in the carbonate rocks from this study. Solid symbols indicate localities where the samples yielded only calcite; hollow symbols denote localities where the calcite contained dolomite inclusions. Fields of primary igneous carbonate (Taylor et al., 1967) and Archean sedimentary carbonate (Veizer et al., 1989) are shown. Black arrows indicate possible changes in isotopic compositions due to 1) decarbonation during metamorphism (Swain et al., 2015); 2) high-T alteration (Demény et al., 2004); 3) low-T alteration (Demény et al., 2004); 4) sediment assimilation (Demény et al., 2004); and 5) degassing or assimilation of biogenic carbon (Lira and Ripley, 1992; Demény et al., 2004). Abbreviations: BX, brecciated variety of carbonate rock at outcrop PCL-01; MT, magnetite-rich variety of carbonate rock at outcrop PCL-01; GH, granite-hosted calcite at outcrop PCL-01; V-PDB, Vienna Peedee belemnite; V-SMOW, Vienna Standard Mean Ocean Water.

### Outcrop PCL-01

Carbonate rocks in the western part of Partridge Crop Lake (Figure GS2017-4-1b) were first reported by Dawson (1952), and were revisited and resampled in 2013 and 2016. The carbonate rocks are developed in the Wintering Lake granite and Archean mafic gneiss as discontinuous bands extending for up to 75 m along the shoreline. Most volumetrically significant are carbonate breccias that comprise a carbonate matrix showing evidence of ductile deformation (folding and flow; Figure GS2017-4-6a) and abundant clasts aligned with the fold axes.

Less common occurrences of carbonate at this locality are a massive carbonate rock rich in serpentinized olivine and magnetite and confined to the contact with a mafic schist, and pegmatitic veins crosscutting the Wintering Lake granite and hosting medium- to coarse-grained calcite (Figure GS2017-4-6b). The folded clast-rich rock contains felsic clasts and xenocrysts, and is crosscut by granitic veins. Major minerals are calcite, diopside and quartz; minor to accessory phases include microcline, chlorite, amphibole, meionite, titanite, clinozoisite, zeolite, magnetite and plagioclase ( $An_{8-39}$ ). Calcite is inequigranular, shows high-strain deformation features and forms embayments in highly altered diopside grains. The massive rock is composed of calcite, phlogopite, serpentinized forsterite, magnetite, dolomite and spinel, with subordinate chlorite, quartz, pargasite (after diopside), gibbsite (after spinel), ilmenite and zircon. Dolomite forms zoned inclusions in calcite that are interpreted

as recrystallized exsolution lamellae and as subhedral grains mantling mafic silicates. Phlogopite is enriched in BaO along the rim (locally up to 6.2 wt. % oxide). The major constituents of the calcite-bearing granitoid veins are albite ( $An_{6-7}$ ; replacing primary plagioclase), quartz, muscovite, chlorite and calcite, with accessory Fe-oxide and relict plagioclase, and trace potassium feldspar and ankerite. Calcite contains abundant inclusions of chlorite and Fe-oxide, and occurs interstitially to the secondary albite-muscovite aggregates.

Calcite from the breccias shows low Sr, Ba and  $\Sigma$ REE abundances in comparison to carbonatites (Figure GS2017-4-3a); its chondrite-normalized REE profiles are characterized by relative enrichment in HREE, a negative Eu anomaly (Figure GS2017-4-4) and Y/Ho ratios that are consistently above the primitive-mantle value (Figure GS2017-4-3b). The granite-hosted calcite has the highest FeO content (2.3–2.7 wt. %) among the studied samples; its Sr abundances are also higher than in the majority of the samples (with the exception of 36-77-435-1), whereas Ba is below detection. Total REE abundances (Figure GS2017-4-3a) are among the lowest measured in this study. Hence, normalized REE profiles and indicator ratios are not available for this sample. The C-O stable-isotope compositions of carbonate from both the brecciated and the olivine-magnetite-rich rocks plot outside the igneous carbonate field toward higher  $\delta^{13}C_{V-PDB}$  and  $\delta^{18}O_{V-SMOW}$  values, whereas the granite-hosted calcite is characterized by a very low  $\delta^{13}C_{V-PDB}$  and high  $\delta^{18}O_{V-SMOW}$  values (Figure GS2017-4-5).

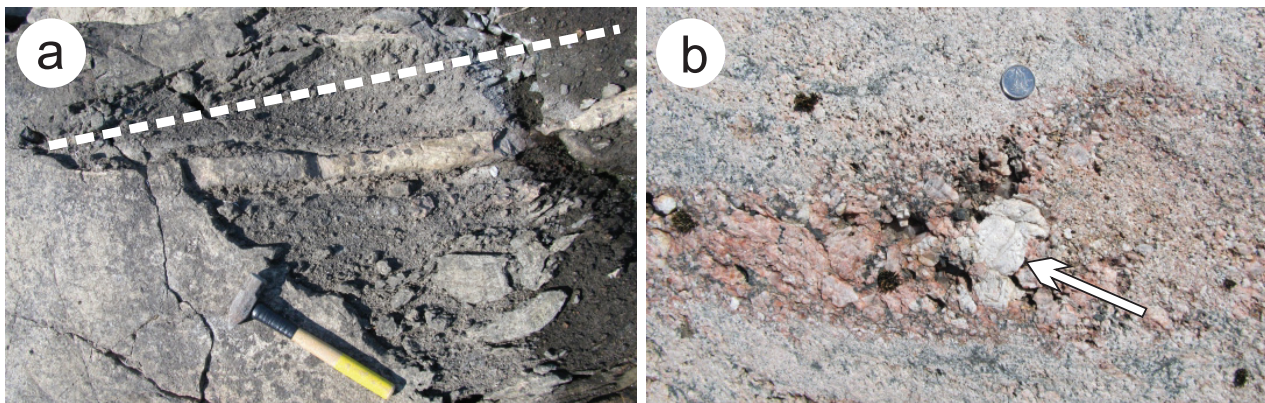


**Figure GS2017-4-6:** Structural and textural relations of the carbonate rock at outcrop PCL-01: **a)** folded and brecciated carbonate rock; note alignment of clasts and vein with fold-axial plane (red dashed line; hammer for scale); **b)** calcite-bearing granite unit; note coarse calcite grain (~6 cm across; red arrow).

The structural relations observed among the carbonate rocks of PCL-01 suggest intrusive emplacement of the matrix-supported breccias. Local contamination with silica-undersaturated material from the mafic schist and late-stage remobilization of  $\text{CO}_2$  would potentially account for the olivine-magnetite-rich facies and calcite-bearing felsic veins, respectively. However, the observed structures and textures do not necessarily imply magma as a source of carbonate (Le Bas et al., 2002, 2004). In the present case, the presence of spinel and meionite implies a metasedimentary origin (Le Bas et al., 2002), which is consistent with the low Sr and REE levels, negative Eu anomaly, elevated Y/Ho ratios and  $\delta^{13}\text{C}_{\text{V-PDB}}$  values, and high  $\delta^{18}\text{O}_{\text{V-SMOW}}$  values in calcite from the clast-rich carbonate rock (Veizer et al., 1989; Le Bas et al., 2002, 2004; Chakhmouradian et al., 2016a). The low  $\delta^{13}\text{C}_{\text{V-PDB}}$  and high  $\delta^{18}\text{O}_{\text{V-SMOW}}$  values in the granite-hosted calcite and its intimate association with metasomatized plagioclase are consistent with partial  $\text{CO}_2$  remobilization from the carbonate breccias during the emplacement of granitic magma.

### Outcrop PCL-02

A large outcrop of layered carbonate-bearing rocks is present on the north side of a large island in the southwestern corner of Partridge Crop Lake (Figure GS2017-4-1b). The outcrop contains several carbonate lenses within a sequence of Archean mafic to ultramafic schists, metapelites, amphibolite and calcsilicate units. The most prominent carbonate unit occurs conformably as vertically stacked boudins with a metapelitic interstitial material, and is bordered by a metapelitic unit to the west and an ultramafic schist to the east. Thin (<4 cm in width) carbonate boudins are present also within the amphibolite and mafic schist. Small-scale isoclinal folds with axial planes parallel to the bedding, as well as repetitive stratigraphy, indicate folding of the sequence. This metamorphic assemblage is crosscut by pegmatite dikes. The carbonate unit comprises predominantly calcite, with dolomite present as exsolution lamellae and rims around mafic-silicate grains. The major silicate phases are serpentinized forsterite, phlogopite, diopside and tremolite. Phlogopite grains are locally enriched in Ba and partially chloritized.

Calcite at PCL-02 contains variable levels of Mg, Fe and Mn. The Sr, Ba and REE abundances in this mineral are much lower than those expected in igneous calcite (Figure GS2017-4-3a), whereas the chondrite-normalized REE profile (Figure GS2017-4-4) is flat and shows a strong negative Eu anomaly. The Y/Ho ratios are consistently above the primitive-mantle value (Figure GS2017-4-3b), but the measured C-O isotope compositions are inconclusive (Figure GS2017-4-5). Dolomite-calcite relationships suggest that the former mineral was overgrown by the latter, or reacted with silicate minerals to yield calcite and Mg-silicates. The low Sr, Ba and REE abundances and indicator REE ratios of the calcite are inconsistent with a magmatic source and imply a metasedimentary origin (Le Bas et al., 2002, 2004; Chakhmouradian et al., 2016a). The low  $\delta^{13}\text{C}_{\text{V-PDB}}$  value could be produced by partial decarbonation during metamorphism and thus agrees with this interpretation. The calcite-dolomite pairs at PCL-02 give a range of equilibrium temperatures clustering between 674°C and 734°C for the calcite with intermediate Mg contents, and between 822°C and 847°C for the high-Mg grains. However, the analyzed high-Mg areas likely incorporate submicroscopic dolomite lamellae, yielding erroneously high T estimates. Hence, the separation of calcite and dolomite is interpreted to have occurred at ~700°C.

### Outcrop PCL-03

This occurrence, located on an island in the southern section of Partridge Crop Lake (Figure GS2017-4-1b), comprises primarily amphibolite crosscut by anastomosing carbonate veins with occasional pockets up to 20 cm across. The fine- to coarse-grained carbonate material filling the veins is locally associated with hornblende. In addition to major calcite, dolomite and amphibole, some of the veins contain accessory diopside, muscovite, clinozoisite, garnet, pyrite and chalcopyrite.

Calcite contains numerous dolomite inclusions. Clinozoisite and muscovite form complete pseudomorphs after an unknown mineral (plagioclase?). Calcite occurs as two distinct varieties that differ in their Fe content yet are similar in their Mg and Mn contents. Dolomite grains overgrown by calcite are

irregularly zoned, with significant variations in Mg, Mn and Fe contents. Barium, Sr and REE levels are low in the calcite, and its chondrite-normalized REE profile displays unusual enrichment in the middle of the lanthanide series, accompanied by a weak positive Eu anomaly (Figure GS2017-4-4). Where both elements could be reliably detected, Y/Ho ratios are close to the primitive-mantle value. The stable-isotope values plot outside the hypothesized field of igneous carbonate (Figure GS2017-4-5). The mineralogical simplicity of carbonate veins at PCL-03, their intimate association with metamorphosed mafic rocks and the composition of their constituent calcite all indicate a noncarbonatic origin and possible genetic links to metamorphism and removal of Ca and other elements (positive Eu anomaly) from precursor igneous plagioclase by CO<sub>2</sub>-rich fluids (Eickmann et al., 2009; Chakhmouradian et al., 2016a).

### Outcrop PCL-04

A similar occurrence of carbonate rocks was reported on an island in the northwestern corner of the southern basin of Partridge Crop Lake by Couëslan (2013; Figure GS2017-4-1b). Here, carbonate veins also clearly postdate their Archean mafic hostrock but were subjected to Paleoproterozoic greenschist-facies retrograde metamorphism. The C isotope composition of calcite is consistent with a mantle source, but its enrichment in heavy O is not, possibly indicating remobilization of carbonate material from the amphibolite by low-T fluids (Demény et al., 2004). The mineralogy of the veins, as well as the absence of any evidence of contact metasomatism in their surrounding amphibolite, suggest a low-T hydrothermal origin.

### Bryce Bay

On an island in Bryce Bay, amphibolite is crosscut by a carbonate vein (Figure GS2017-4-1b). The vein is ~50 cm wide and contains calcite and orange calcic garnet. The calcite lacks detectable Mg or Fe, and concentrations of Mn, Sr and REE are among the lowest in the sample suite examined during this study (Figure GS2017-4-3a), so none of the indicator REE ratios could be calculated. Although the measured  $\delta^{13}\text{C}_{\text{V-PDB}}$  and  $\delta^{18}\text{O}_{\text{V-SMOW}}$  values (Figure GS2017-4-5) plot just outside the range for igneous carbonate, the low trace-element levels of the Bryce Bay calcite and its association with calcic garnet suggest a contact-metamorphic origin. Skarns with similarly low  $\delta^{13}\text{C}_{\text{V-PDB}}$  and  $\delta^{18}\text{O}_{\text{V-SMOW}}$  values have been reported in the literature (e.g., Sahlström, 2014).

### Outcrop NL-01

This occurrence, initially reported by Dawson (1952), is situated approximately 1 km east of the channel connecting Natawahunan and Partridge Crop Lakes (Figure GS2017-4-1b). The carbonate rock occurs semiconformably within tonalitic basement gneiss and is separated by a calcsilicate unit from pegmatitic granite that crosscuts the gneiss. The carbonate unit hosts granite clasts, which are concentrically mantled by calcsilicate material and a phlogopite-rich rim, as well as folded boudins composed predominantly of diopside with a phlogopite rim (Figure GS2017-4-7a).

The carbonate unit is mineralogically heterogeneous and can be subdivided into two lithological types: forsterite-calcitic and dolomite-calcitic. The former rock type is composed

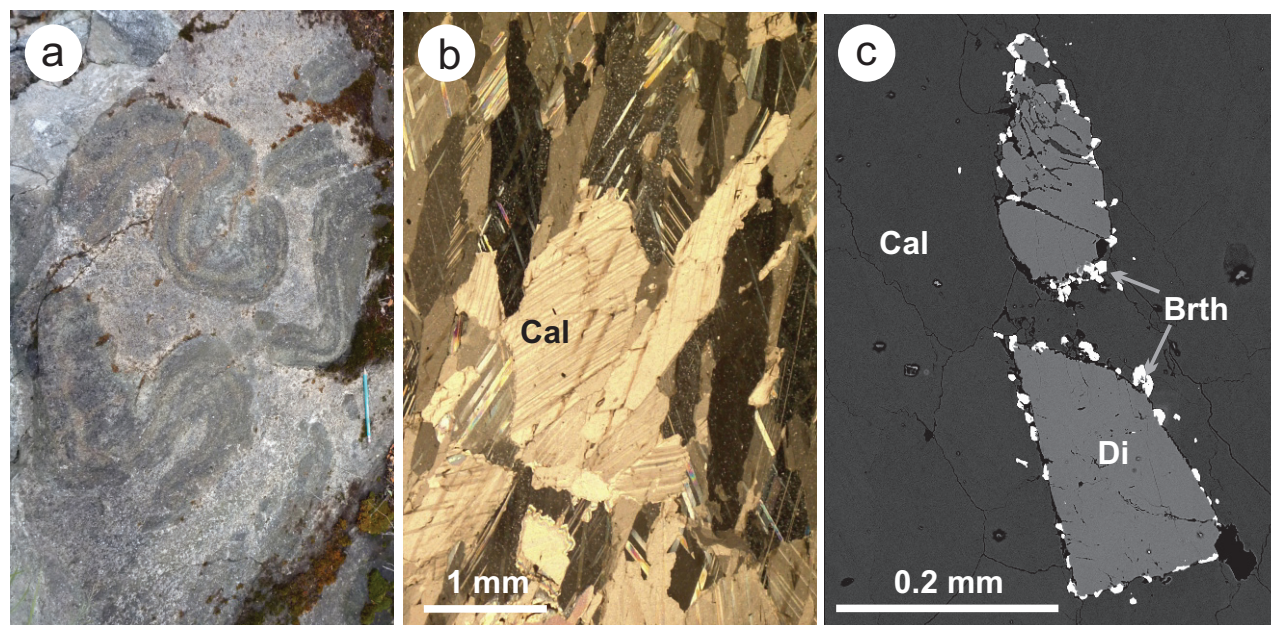


**Figure GS2017-4-7:** Textural characteristics of the carbonate rocks from Natawahunan Lake: **a)** folded diopside-phlogopite boudins hosted in carbonate unit (outcrop NL-01; pencil approximately 20 cm); **b)** unidirectionally oriented, elongate and polysynthetically twinned calcite grains (outcrop NL-02); **c)** backscattered-electron scanning electron microscope (BSE) image of diopside with discontinuous britholite rim (NL float). Abbreviations: Cal, calcite; Di, diopside, Brth, britholite.

predominantly of calcite, serpentinized forsterite and chlorite, whereas accessory phases are magnetite, dolomite, tremolite and barite. Calcite forms the inequigranular groundmass and contains zoned dolomite inclusions interpreted as exsolution lamellae. The second rock type is very heterogeneous in modal composition and consists primarily of calcite, dolomite, diopside, forsterite, phlogopite, tremolite, serpentine and magnetite with accessory chlorite (after phlogopite), plagioclase, pyrrhotite, apatite and barite. In this rock, calcite is similar to that in the forsterite-calcitic type, whereas dolomite also occurs as subhedral rims on silicate phases, where it is associated with magnetite and succeeded by interstitial calcite. In common with the carbonate rocks from outcrop PCL-01, phlogopite at NL-01 is zoned and locally enriched in Ba.

Both examined rock types contain calcite with elevated Mg and Mn levels relative to the majority of other samples in this study. Strontium, Ba and REE abundances, and  $(La/Yb)_{CN}$  ratios, are lower than expected for igneous calcite (Figure GS2017-4-3a), and chondrite-normalized REE distributions display an unusual U-shaped profile (Figure GS2017-4-4). There appears to be a small negative Eu anomaly (although  $Eu/Eu^*$  can be calculated only for a few analyses), whereas the calculated Y/Ho values are mostly above the primitive-mantle value. The calculated temperatures of calcite-dolomite exsolution range from 654 to 742°C. Mixed carbonate samples yield relatively high  $\delta^{13}C_{V-PDB}$  and  $\delta^{18}O_{V-SMOW}$  values that are well outside the igneous carbonate range (Figure GS2017-4-5). Based on these compositional and petrographic characteristics, these rocks are interpreted as a lower-granulite-facies ( $M_2$ ) silicate-carbonate assemblage (e.g., Bucher and Grapes, 2011) that has been subjected to multistage retrograde metamorphism, as reflected in complex replacement and overgrowth textures.

### Outcrop NL-02

Carbonate rocks also occur ~200 m west of the NL-01 outcrop (Figure GS2017-4-1b) as a bifurcating network of veins ~7 m wide that incorporates relict fragments of calcsilicate and pegmatitic material. A phlogopite-rich selvage is present between the carbonate unit and mafic-volcanic country rocks. The carbonate assemblages at this occurrence are highly variable in texture and mineralogy, and contain clasts of several different types. The major constituent minerals are calcite, forsterite, diopside, meionite, phlogopite and serpentine, with accessory magnetite, chlorite, clinozoisite, epidote, grossular, plagioclase, pyrite, spinel, barite and anhydrite. Calcite is the only carbonate mineral observed in the unit and ranges from coarse, elongate grains (Figure GS2017-4-7b) with inclusions of barite and anhydrite to fine, equant grains that infill embayments in silicate phases. Fine- to coarse-grained diopside is ubiquitous across the carbonate unit and is commonly mantled by zoned garnet. Another common reaction product is clinozoisite, which locally grades into epidote intergrown with grossular.

Calcite from outcrop NL-02 contains no detectable Mg, and Mn and Fe values are lower than those in NL-01. Its Sr

content is very low, but Ba and REE abundances are higher than in the majority of other samples examined in this study, with the exception of the Split Lake material (Figure GS2017-4-3a). Note that at least some of the measured Ba is probably due to subsurface barite inclusions sampled during laser ablation. The chondrite-normalized REE profile exhibits some enrichment in LREE and a distinct negative Eu anomaly, and level off beyond Gd (Figure GS2017-4-4). In common with the NL-01 samples, this calcite is characterized by elevated Y/Ho ratios (Figure GS2017-4-3b) and relatively heavy C-O isotope compositions (Figure GS2017-4-5). Many geochemical and mineralogical similarities between the carbonate assemblages at the two outcrops suggest that they share a petrogenetic history, but the abundance of Al-rich phases (meionite, grossular, clinozoisite and epidote) and the REE characteristics of calcite at NL-02 imply the presence of a significant pelitic component in its protolith (Bucher and Grapes, 2011; Grizelj et al., 2017).

### NL float

In addition to the two outcrops, several angular carbonate cobbles were found on a beach on Natawahunan Lake (Figure GS2017-4-1a) by C. Couëslan. Although their source could not be located, the occurrence of these cobbles in proximity to one another and their angular shape suggest that they were locally derived. Equigranular, evenly distributed calcite constitutes the bulk of this rock; other major minerals are diopside, garnet and meionite. Accessory phases include quartz, chlorite, serpentine, wollastonite, britholite, apatite and microcline. Quartz and wollastonite occur in clasts, whereas garnet is zoned from grossular to andradite and occurs as rims on silicate minerals, pseudomorphs after diopside and euhedral grains with poikilitic rims hosting calcite inclusions. Britholite occurs as minute crystals (<30  $\mu$ m) intergrown with andradite to form discontinuous rims on diopside and meionite, and as 'necklaces' of such crystals around diopside grains (Figure GS2017-4-7c). A single resorbed grain of apatite mantled by britholite was observed in the calcite matrix.

The calcite in the carbonate cobbles contains low Mg and Mn but elevated Sr and REE relative to the majority of the samples studied (Figure GS2017-4-3a). The chondrite-normalized REE profile shows enrichment in LREE (Figure GS2017-4-4). Of the indicator REE ratios, only Y/Ho could be calculated for some of the laser-ablation measurements and is consistently lower than the primitive-mantle value. The relative enrichment of calcite in LREE and light C and O isotopes (Figure GS2017-4-5) is similar to that found in carbonatitic samples. The Sr content and Y/Ho value are too low for igneous calcite but comparable to those reported for hydrothermal calcite associated with some carbonatites (Chakhmouradian et al., 2016a). The observed mineralogical characteristics are also difficult to reconcile with an igneous source. Although britholite is present and has been described in retrogressively metamorphosed carbonatites (Zaitsev and Chakhmouradian, 2002; Ahijado et al., 2005), this mineral has also been reported as a replacement product after primary REE-bearing phases in some skarns (e.g.,

Smith et al., 2002). The abundance of calcic garnets, meionite and wollastonite in the NL float is characteristic of skarns.

### **Pie Lake**

This occurrence (Figure GS2017-4-1b) is represented by an outcrop of sheared quartz metawacke with minor metapelite, which are locally retrogressed to greenschist facies. Calcite occurs pervasively within an ~1 m wide mylonitic zone developed in the metawacke concordant with the regional metamorphic banding. The examined metawacke sample is texturally heterogeneous owing to mylonitization and associated redistribution of quartz and other minerals into modally distinct domains. The sample is composed of fine-grained, mosaic-textured quartz associated with fine-grained, sub- to anhedral garnet and interstitial calcite. The garnet is zoned from grossular in the core to andradite in the discontinuous rim, whereas calcite occurs interstitially to clinozoisite and increases in abundance and grain size in the quartz-rich domains. Diopside, amphibole and titanite are observed as fractured grains associated with the mosaic quartz.

The calcite contains no detectable Mg or Fe. The measured Sr and REE abundances are among the lowest observed in this study (Figure GS2017-4-3a), so the chondrite-normalized profile is incomplete (Figure GS2017-4-4). Only one analysis gave a meaningful Y/Ho ratio, which is below the primitive-mantle value. The calcite plots within the range of  $\delta^{13}\text{C}_{\text{V-PDB}}$  and  $\delta^{18}\text{O}_{\text{V-SMOW}}$  values typical of igneous carbonate (Figure GS2017-4-5). The mylonitic texture of the carbonate unit is not diagnostic of any specific process because strain is typically partitioned into carbonate rocks, which are generally more ductile than their host silicate units (Chakhmouradian et al., 2016b). Although the C-O isotope composition of the Pie Lake calcite is 'carbonatite-like', the extremely low levels of Sr, Ba and REE in this mineral and the absence of any accessory phases characteristic of carbonatites argue against an igneous origin for the host mylonitic rock or its protolith.

### **Discussion**

Of the 10 occurrences examined during this study, only one (sample 36-77-435-1, collected by T. Corkery at Split Lake in 1977) can be classified as carbonatite with a reasonable degree of confidence. The calcite from this occurrence meets all of the trace-element and stable-isotope criteria for igneous carbonate but shows clear evidence of subsolidus re-equilibration with metamorphic (?) fluids (i.e., secondary zoning involving the loss of REE). Notably, however, the trace-element patterns observed in sample 36-77-435-1 differ significantly from those documented in the material collected in 2016. Although hydrothermal processes can potentially account for the observed geochemical variations, a further detailed isotopic investigation of the available material and mapping at Split Lake are needed to establish the provenance of carbonate in this part of the SLB and explore possible geodynamic implications of these findings.

The remaining nine occurrences range from indisputable, high-grade carbonate-silicate assemblages, whose mineralogical

complexity reflects the prolonged metamorphic history of the PGD (e.g., outcrop NL-01), to less unequivocal cases where petrogenetic interpretation is impossible in the absence of further data (e.g., NL float). One important outcome of this study is that it demonstrates extensive compositional variations in carbonates of nonigneous origin. From the data presented in this report (Figures GS2017-4-3 to -5), it is clear that no single geochemical criterion can be reliably used to identify the source of carbonate in deformed Precambrian rocks. Specific trace-element and stable-isotope ratios may have limited utility when it comes to metamorphic assemblages that underwent decarbonation and fluid-assisted element remobilization. It is also noteworthy that the inferred metasedimentary carbonate rocks at outcrops PCL-01, PCL-02 and NL-01 contain Ba-rich phlogopite (some with as much as 6.2 wt. % BaO), which implies that Ba was either liberated from an authigenic host (e.g., barite) during metamorphism or introduced with a metamorphic fluid from an external source (Bol et al., 1989). Barium-rich phlogopite is common in alkaline igneous rocks and carbonatites (e.g., Edgar, 1992; Reguir et al., 2009) but relatively rare in metasedimentary rocks. Although it is possible that unusual conditions may be required to stabilize this mineral in high-grade marbles (Bol et al., 1989), an equally likely explanation is the low solubility of barite in fluids and the paucity of potential external sources that could supply fluid-borne Ba (such as carbonatitic magma). The petrogenetic implications of Ba in micas from the PGD rocks remain to be ascertained.

The association of calcite and dolomite in some of the examined rocks allows for the temperature of calcite-dolomite equilibration to be determined (Anovitz and Essene, 1987). The temperatures calculated for the southern basin of Partridge Crop Lake (PCL-02) and Natawahunan Lake (NL-01) are similar, i.e., ~670–730 and 650–740°C, respectively. These estimates are ~100°C lower than the peak metamorphic conditions proposed in the literature (Heaman et al., 2011). Thus, calcite-dolomite exsolution probably occurred during retrograde metamorphism at the amphibolite-facies conditions, as described in Couëslan (2016). Geothermometric calculations can be performed for carbonate inclusions in metamorphic porphyroblasts (e.g., forsterite) and used to study prograde metamorphic processes in granulite-facies terranes (Mizuochi et al., 2010). Calcite or dolomite inclusions do occur in forsterite from the PCL-01, PCL-02, and NL-01 carbonate rocks and, in combination with exsolved calcite-dolomite intergrowths in the groundmass, provide ample opportunity for future work on the metamorphic history of the PGD.

### **Economic considerations**

Rare-earth elements are becoming increasingly relevant as a commodity because their supply is currently limited geographically, whereas the number of technological applications dependent on REE materials, and the volume of industrial production arising from these technologies, have been increasing continuously during the past three decades (Chakhmouradian and Wall, 2012). Carbonatites are of great economic significance as the principal natural source of REE (Chakhmouradian

and Wall, 2012); these rocks host, or are genetically associated with, the world's largest rare-earth deposits (e.g., Mao-niuping, Daluxiang, and Bayan Obo deposits, China; Xu et al., 2010; Chakhmouradian and Wall, 2012; Kynicky et al., 2012). In Canada, a number of initiatives have been launched with support from the Federal Government to secure a domestic supply of these increasingly important commodities (Simandl et al., 2012). The results of the present work and recent discoveries of carbonatites and related mantle-derived rocks in the north-western Superior craton of Manitoba (Anderson et al., 2012; Anderson, 2016) indicate the potential for as-yet untapped rare-earth deposits in this part of the province.

## Acknowledgments

The authors thank P. Yang, N. Ball and M. Yun (University of Manitoba) for support with acquisition of analytical data; E. Anderson and N. Brandson for logistical field support; Wings over Kississing for air support; and the Manitoba Hydro Split Lake boat crew for navigational support. A special thanks is extended to T. Martins for organizing the excursion to Split Lake.

## References

- Ahijado, A., Casillas, R., Nagy, G. and Fernández, C. 2005: Sr-rich minerals in a carbonatite skarn, Fuerteventura, Canary Islands (Spain); *Mineralogy and Petrology*, v. 84, p. 107–127.
- Anders, E. and Grevesse, N. 1989: Abundances of the elements: meteoric and solar; *Geochimica et Cosmochimica Acta*, v. 53, p. 197–214.
- Anderson, S.D. 2016: Alkaline rocks at Oxford Lake and Knee Lake, northwestern Superior province, Manitoba (NTS 53L13, 14, 15): preliminary results of new bedrock mapping and lithogeochemistry; *in Report of Activities 2016, Manitoba Growth, Enterprise and Trade, Manitoba Geological Survey*, p. 16–27.
- Anderson, S.D., Kremer, P.D. and Martins, T. 2012: Preliminary results of bedrock mapping at Oxford Lake, northwestern Superior Province, Manitoba (parts of NTS 53L12, 13, 63I9, 16); *in Report of Activities 2012, Manitoba Innovation, Energy and Mines, Manitoba Geological Survey*, p. 6–22.
- Anovitz, L.M. and Essene, E.J. 1987: Phase equilibria in the system  $\text{CaCO}_3\text{-MgCO}_3\text{-FeCO}_3$ ; *Journal of Petrology*, v. 28, p. 389–414.
- Böhm, C.O. 1998: Geology of the Natawahunan Lake area; *in Report of Activities 1998, Manitoba Energy and Mines, Geological Services*, p. 56–59.
- Böhm, C.O., Heaman, L.M. and Corkery, M.T. 1999: Archean crustal evolution of the northwestern Superior Province margin: U-Pb zircon results from the Split Lake Block; *Canadian Journal of Earth Sciences*, v. 36, p. 1973–1987.
- Bol, L.C.G.M., Bos, A., Sauter, P.C.C. and Jansen, J.B.H., 1989: Barium-titanium-rich phlogopites in marbles from Rogaland, southwest Norway; *American Mineralogist*, v. 74, p. 439–447.
- Bucher, K. and Grapes, R. 2011: *Petrogenesis of Metamorphic Rocks*; Springer-Verlag, Berlin, 441 p.
- Chakhmouradian, A.R. 2006: High-field-strength elements in carbonatitic rocks: geochemistry, crystal chemistry and significance for constraining sources of carbonatites; *Chemical Geology*, v. 235, p. 18–160.
- Chakhmouradian, A.R. and Wall, F. 2012: Rare earth elements: minerals, mines, magnets (and more); *Elements*, v. 8, p. 333–340.
- Chakhmouradian, A.R., Böhm C.O., Demény, A., Reguir, E.P., Hegner, E., Creaser, R.A., Halden, N.M. and Yang, P. 2009a: “Kimberlite” from Wekusko Lake, Manitoba: actually a diamond-indicator-bearing dolomite carbonatite; *Lithos*, v. 112, p. 347–357.
- Chakhmouradian, A.R., Couëslan, C.G. and Reguir, E.P. 2009b: Evidence for carbonatite magmatism at Paint Lake, Manitoba (parts of NTS 63O8, 63P5, 12); *in Report of Activities 2009, Manitoba Innovation, Energy and Mines, Manitoba Geological Survey*, p. 118–126.
- Chakhmouradian, A.R., Reguir, E.P., Kressall, R.D., Crozier, J., Pisiak, L.K., Sidhu, R. and Yang P. 2015: Carbonatite-hosted niobium deposit at Aley, northern British Columbia (Canada): mineralogy, geochemistry and petrogenesis; *Ore Geology Reviews*, v. 64, p. 642–666.
- Chakhmouradian, A.R., Reguir, E.P., Couëslan, C. and Yang, P. 2016a: Calcite and dolomite in intrusive carbonatites. II. trace-element variations; *Mineralogy and Petrology*, v. 110, p. 361–377.
- Chakhmouradian, A.R., Reguir, E.P. and Zaitsev, A. 2016b: Calcite and dolomite in intrusive carbonatites. I. textural variations; *Mineralogy and Petrology*, v. 110, p. 333–360.
- Couëslan, C.G. 2008: Preliminary results from geological mapping of the west-central Paint Lake area, Manitoba (parts of NTS 63O8, 9, 63P5, 12); *in Report of Activities 2008, Manitoba Science, Technology, Energy and Mines, Manitoba Geological Survey*, p. 99–108.
- Couëslan, C.G. 2013: Preliminary results from bedrock mapping in the Partridge Crop Lake area, eastern margin of the Thompson nickel belt, central Manitoba (parts of NTS 63P11, 12); *in Report of Activities 2013, Manitoba Mineral Resources, Manitoba Geological Survey*, p. 34–45.
- Couëslan, C.G. 2014: Preliminary results from bedrock mapping in the Partridge Crop Lake area, eastern margin of the Thompson nickel belt, central Manitoba (parts of NTS 63P11, 12); *in Report of Activities 2014, Manitoba Mineral Resources, Manitoba Geological Survey*, p. 18–31.
- Couëslan, C.G. 2016: Preliminary results of bedrock mapping in the Natawahunan Lake area, western margin of the Pikwitonei granulite domain, central Manitoba (parts of NTS 63P11, 14); *in Report of Activities 2016, Manitoba Growth, Enterprise and Trade, Manitoba Geological Survey*, p. 28–39.
- Dawson, A.S. 1952: *Geology of the Partridge Crop Lake area*, Cross Lake Mining Division, Manitoba; Manitoba Department of Mines and Natural Resources, Mines Branch, Publication 41-1, 26 p.
- Demény, A., Sitnikova, M.A. and Karchevsky, P.I. (2004): Stable C and O isotope compositions of carbonatite complexes of Kola Alkaline Province: phoscorite-carbonatite relationships and source compositions; *in Phoscorites and Carbonatites from Mantle to Mine: the Key Example of the Kola Alkaline Province*, F. Wall and A.N. Zaitsev (ed.), Mineralogical Society of Great Britain and Ireland, London, Mineralogical Society Series, no. 10, p. 407–431.
- Edgar, A.P. 1992: Barium-rich phlogopite and biotite from some Quaternary alkali mafic lavas, West Eifel, Germany; *European Journal of Mineralogy*, v. 4, p. 321–330.
- Eickmann, B., Bach, W., Rosner, M. and Peckmann, J. 2009: Geochemical constraints on the modes of carbonate precipitation in peridotites from the Logatchev Hydrothermal Vent Field and Gakkell Ridge; *Chemical Geology*, v. 268, p. 97–106.
- Grizelj, A., Peh, Z., Tibljaš, D., Kovačić, M. and Kurečić, T. 2017: Mineralogical and geochemical characteristics of Miocene pelitic sedimentary rocks from the southwestern part of the Pannonian Basin System (Croatia): implications for provenance studies; *Geoscience Frontiers*, v. 8, p. 65–80.
- Halls, H.C. and Heaman, L.M. 2000: The paleomagnetic significance of new U-Pb age data from the Molson dyke swarm, Cauchon Lake area, Manitoba; *Canadian Journal of Earth Sciences*, v. 37, p. 957–966.

- Hartlaub, R.P., Böhm, C.O., Heaman, L.M. and Simonetti, A. 2005: Northwestern Superior craton margin, Manitoba: an overview of Archean and Proterozoic episodes of crustal growth, erosion and orogenesis (parts of NTS 54D and 64A); *in* Report of Activities 2005, Manitoba Industry, Economic Development and Mines, Manitoba Geological Survey, p. 54–60.
- Hartlaub, R.P., Heaman, L.M., Böhm, C.O. and Corkery, M.T. 2003: Split Lake Block revisited: new geological constraints from the Birthday to Gull Rapids corridor of the lower Nelson River (NTS 54D5 and 6); *in* Report of Activities 2003, Manitoba Industry, Trade and Mines, Manitoba Geological Survey, p. 114–117.
- Heaman, L.M. and Corkery, T. 1996: U-Pb geochronology of the Split Lake Block, Manitoba: preliminary results; LITHOPROBE Trans-Hudson Orogen Transect, Report of Sixth Transect Meeting, Saskatoon, Saskatchewan, April 1–2, 1996, LITHOPROBE Secretariat, University of British Columbia, Vancouver, British Columbia, Report 55, p. 60–68.
- Heaman, L.M., Böhm, C.O., Machado, N., Krogh, T.E., Weber, W. and Corkery, M.T. 2011: The Pikwitonei Granulite Domain, Manitoba: a giant Neoproterozoic high-grade terrane in the northwest Superior Province; *Canadian Journal of Earth Sciences*, v. 48, p. 205–245.
- Kuiper, Y.D., Lin, S. and Böhm C.O., 2011: Himalayan-type escape tectonics along the Superior Boundary Zone in Manitoba, Canada; *Precambrian Research*, v. 187, p. 248–262.
- Kynicky J., Smith M.P. and Xu C. 2012: Diversity of rare earth deposits: the key example of China; *Elements* v. 8, p. 361–367.
- Le Bas, M.J. 2008: Fenites associated with carbonatites; *Canadian Mineralogist*, v. 46, p. 915–932.
- Le Bas, M.J., Ba-tttat, M.A.O., Taylor, R.N., Milton, J.A., Windley, B.F. and Evins, P.M. 2004: The carbonatite-marble dykes of Abyan Province, Yemen Republic: the mixing of mantle and crustal carbonate materials revealed by isotope and trace element analysis; *Mineralogy and Petrology*, v. 82, p. 105–135.
- Le Bas, M.J., Subbaro, K.V. and Walsh, J.N. 2002: Metacarbonatite or marble? – the case of the carbonate, pyroxenite, calcite-apatite rock complex at Borra, Eastern Ghats, India; *Journal of Asian Earth Sciences*, v. 20, p. 127–140.
- Lira, R. and Ripley, E.M. 1992: Hydrothermal alteration and REE-Th mineralization at the Rodeo de Los Molles deposit, Las Chacras batholith, central Argentina; *Contributions to Mineralogy and Petrology*, v. 110, p. 370–386.
- Macdonald, J.A., Chakhmouradian, A.R., Couëslan, C.G. and Reguir, E.P. 2017: Stable C and O isotope and major- and trace-element data, with calcite-dolomite equilibration geothermometry, for genetically diverse carbonate rocks in the Pikwitonei granulite domain and Split Lake block (parts of NTS 63P11, 12, 64A1); Manitoba Growth, Enterprise and Trade, Manitoba Geological Survey, Data Repository Item DRI2017005, Microsoft® Excel® file.
- Machado, N., Gapais, D., Potrel, A., Gauthier, G. and Hallot, E. 2011a: Chronology of transpression, magmatism, and sedimentation in the Thompson Nickel Belt (Manitoba, Canada) and timing of Trans-Hudson Orogen–Superior Province collision; *Canadian Journal of Earth Sciences*, v. 48, p. 295–324.
- Machado, N., Heaman, L.M., Krogh, T.E., Weber, W. and Corkery, M.T. 2011b: Timing of Paleoproterozoic granitoid magmatism along the northwestern Superior Province margin: implications for the tectonic evolution of the Thompson Nickel Belt; *Canadian Journal of Earth Sciences*, v. 48, p. 325–346.
- Mezger, K., Bohlen, S.R. and Hanson, G.N. 1990: Metamorphic history of the Archean Pikwitonei Granulite Domain and the Cross Lake Subprovince, Superior Province, Manitoba, Canada; *Journal of Petrology*, v. 31, p. 483–517.
- Mizuochi, H., Satish-Kumar, M., Motoyoshi, Y. and Michibayashi, K. 2010: Exsolution of dolomite and application of calcite-dolomite geothermometry in high-grade marbles: an example from Skallevikshalsen, East Antarctica; *Journal of Metamorphic Petrology*, v. 28, p. 509–526.
- Paktunç, A.D. and Baer, A.J. 1986: Geothermobarometry of the northwestern margin of the Superior Province: implications for its tectonic evolution; *Journal of Geology*, v. 94, p. 381–394.
- Reguir, E.P., Chakhmouradian, A.R., Halden, N.M., Malkovets, V.G. and Yang, P. 2009: Major- and trace-element compositional variation of phlogopite from kimberlites and carbonatites as a petrogenetic indicator; *Lithos*, v. 112S, p. 372–384.
- Sahlström, F. 2014: Stable isotope systematics of skarn-hosted REE-silicate-magnetite mineralisations in central Bregslagen, Sweden; M.Sc. thesis, Uppsala University, Sweden, 82 p.
- Simandl, G.J., Prussin, E.A. and Brown, N. 2012: Specialty metals In Canada; *British Columbia Geological Survey, Open File 2012-7*.
- Smith, M.P., Henderson, P. and Jeffries, T. 2002: The formation and alteration of allanite in skarn from the Beinn an Dubhaich granite aureole, Skye; *European Journal of Mineralogy*, v. 14, p. 471–486.
- Swain, S.K., Sarangi, S., Srinivasan, R., Sarkar, A., Bhattacharya, S., Patel, S.C., Pasayat, R.M. and Sawkar, R.H. 2015: Isotope (C and O) composition of auriferous quartz carbonate veins, central lode system, Gadag Gold Field, Dharwar Craton, India: implications to source of fluids; *Ore Geology Reviews*, v. 70, p. 305–320.
- Taylor, H.P., Frechen, J. and Degens, E.T. 1967: Oxygen and carbon isotope studies of carbonatites from the Laacher See District, West Germany and the Alnö District, Sweden; *Geochimica et Cosmochimica Acta*, v. 31, p. 407–430.
- Veizer, J., Hoefs, J., Lowe, D.R. and Thurston, P.C. 1989: Geochemistry of Precambrian carbonates: II. Archean greenstone belts and Archean sea water; *Geochimica et Cosmochimica Acta*, v. 53, p. 859–871.
- Weber, W. 1978: Natawahunan Lake (NTS 63P10, 11, 15 and parts of 64P12, 14, and 64A2); *in* Report of Field Activities 1978, Manitoba Energy and Mines, Mineral Resources Division, p. 47–53.
- Xu, C., Campbell, I.H., Allen, C.M., Huang, Z., Qi, L., Zhang, H. and Zhang, G. 2007: Flat rare-earth element patterns as an indicator of cumulate processes in the Lesser Qinling carbonatites, China; *Lithos*, v. 95, p. 267–278.
- Xu, C., Wang, L., Song, W. and Wu, M. (2010) Carbonatites in China: a review for genesis and mineralization; *Geoscience Frontiers*, v. 1, p. 105–114.
- Zaitsev, A.N. and Chakhmouradian, A.R. 2002: Calcite-amphibole-clinopyroxene rock from the Afrikanda complex, Kola Peninsula, Russia: mineralogy and a possible link to carbonatites. II. Oxy salt minerals; *Canadian Mineralogist*, v. 40, p. 103–120.